Clinical Surgery Journal

Research Article | Vol 5 Iss S13

Synthesis, Characterization, and Biological Evaluation of Copper Nanoparticles using Palm (*Borassus flabellifer L*) Nectar as Bio-Reductant

Anbalagan Srinivasan[1], Kamaludeen Balkis Ameen[2], Krishnan Rajasekar[3], Perumal Pandaram[4], Samia Attia Negm[5], Amal Ali Bahafi[5], S. Arivalagan[5] and Alagunambi Ramasubbu[1*]

[1]*Department of Chemistry, Government Arts College (Autonomous), Tamil Nadu, India*

[2]*Herbiomes Pvt. India Limited, Tamil Nadu, India*

[3]*Department of Nanotechnology, Anna University Regional Campus, Tamil Nadu, India*

[4]*Thermoluminescent Dosimeter Lab, Kudankulam Nuclear Power Project, Tamil Nadu, India*

[5]*Department of Physics, Department of Analytical Chemistry, Ibn Sina Medical College, Kingdom of Saudi Arabia*

Correspondence should be addressed to Alagunambi Ramasubbu, Post Graduate and Research Department of Chemistry, Government Arts College (Autonomous), Coimbatore – 641 018, Tamil Nadu, India

Received: July 19, 2022; Accepted: July 26, 2022; Published: August 01, 2022

ABSTRACT

The present study elucidates the eco-benign synthesis of Copper Nanostructures (Cu-NS) using Palm Nectar (PN) as a bio-reductant besides stabilizing the nascent Cu-NS germinate. The Palm Nectar supported Copper Nanostructures (PN-Cu-NS) was subjected to various physicochemical characterization viz., UV-Vis. Spectrophotometry, FT-IR, Powder XRD, FE-SEM, EDX, and HR-TEM with SAED pattern. The UV-Vis absorption spectra of the colloidal PN-Cu-NS showed a discrete SPR band at 583 nm with a band gap energy of 2.12 eV, which is corroborated by Diffuse Reflectance Spectra (DRS; band gap = 2.17 eV). The FT-IR vibrational frequencies between 1900 cm^{-1} - 1600 cm^{-1} indicated the presence of carbonyl C=O/C=N/-C=C-/moieties present in the system supporting the role of PN as stabilizing as well as reducing agent. This enables the dual role of PN viz., stabilizing as well as the reducing agent. The X-Ray diffractogram obtained from powder XRD (p-XRD) analysis confirmed the formation of cubic phase of nanocrystalline Cu along with contemporaneous of Cu_2O and the CuO systems. The FE-SEM and HR-TEM micrographic images endorsed the smooth and spherical morphology of PN-Cu-NS. The lattice fringes obtained from HR-TEM micrographs clearly depicted the 'd' spacing value at 0.2 nm attested the Cu (111) phase which is closely related to the value obtained from p-XRD and Selected Area Electron Diffraction (SAED) pattern. Energy dispersive X-ray (EDX) designated the high intense elemental Copper and low intense oxygen; clearly showing the purity of synthesized samples. The DPPH free radical scavenging ability of Synthesized PN-Cu-NS clearly depicted the antioxidant properties. Antimicrobial efficacy of PN-Cu-NS was evaluated against both Gram positive (Staphylococcus aureus, Bacillus subtilis) and Gram negative (*Escherichi coli*, *Pseudomonas aeruginosa*) bacterial strains. The fungi such as *Candida albicans, Aspergillus niger, Aspergillus fumigates* and *Monococeus purpureces* were used to explore the anti-fungal potential of PN-Cu-NS. The cytotoxicity of PN-Cu-NS was assessed against both lung cancer (A549) and Cervical cancer

Citation: Anbalagan Srinivasan, Synthesis, Characterization, and Biological Evaluation of Copper Nanoparticles using Palm (Borassus flabellifer L) Nectar as Bio-Reductant. Clin Surg J 5(S13): 14-28.

(HeLa) cells by MTT assay, and the IC50 value of PN-Cu-NS was found to be a very low quantity of 12 ± 1.2 µg/ml against lung cancer (A549) cells, and 89 µg/ml against HeLa cells, which support the anticancer potential of PN-Cu-NS.

KEYWORDS

Green synthesis; Copper nanostructures; Antioxidant; Cervical cancer cells; Lung cancer cells; Antimicrobial efficacy

INTRODUCTION

Nanoparticles have gained curiosity in modern years due to their incredible potentials in various fields. Consistently, metal and metal oxide nanoparticles have received more attention in biomedical sector, due to their ability to interact with live cells and being antimicrobial [1-4]. Among various metals, Copper nanoparticles fascinating for their cost friendliness, easy accessibility, and unique properties [5-8]. Various chemical and physical methods have been used for synthesis of metallic Copper nanoparticles [9]. However, these strategies are accompanied by many issues including use of harmful solvents, hazardous derivatives and high energy utilization [10-13]. Hence, there is an important need to build up eco-benign approach for the synthesis of metallic nanoparticles [14-16]. A hopeful approach to achieve this goal is to widen the range of biological resources in nature. Certainly, over the several years, microbiological organisms viz., algae, fungi, and bacteria have been used for fabrication of low-cost, potential metallic Copper nanoparticles [17-24]. The main drawback of this microbiological process is the difficulty to maintain viable and active cell culture. To overcome this drawback, plant extracts were used for the synthesis of nanoparticles. In general, plant extracts contain many polyphenolic compounds that could act as capping agents and prevented agglomeration of nanoparticles [25-32]. This eco-benign approach for synthesis is appropriate for large scale synthesis of Copper NPs in health-related applications. Many shrubs and plants were used to synthesize copper nanoparticles such as *Eryngium caucasicum* [16], *Jatropha curcas* [29], *Magnolia grandiflora* [25], *Lantana camara* [26], *Cassia fistula* [27], *Celastrus paniculatus* [28], *Prunus nepalensis* [30], *Cassytha filiformis L*. [5], *Carica papaya* [31] and *Citrus sinensis* [32].

United States Centers for Disease Control and Prevention (CDC) have affirmed that the microbial infections and their drug resistance in microorganisms are a severe peril to animal and human health. Resistance in microorganisms to various antibiotics has been increasing gradually, and many species or strains of microorganisms have developed resistance to one or more antimicrobial agents; Therefore, we need to discover and develop novel strategic, and innovative antimicrobial agents for the control and prevention of microbial infections [2]. Considering this, metallic nanoparticles with surface modifications possibly will offer optimistic applications. The bacterial pathogens are associated with complicated diseases, such as urinary tract infections bacteremia, soft tissue, and respiratory infections [23, 33]. Besides the bacterial strains, the fungal pathogens tend to cause threat to living systems [27, 28]. In addition to the microbial infections, cancer causes fatality greatly around the globe every year. The anticancer therapeutics involving green nanoparticles often synergistically act in combating cancer with fewer side effects, in both *in-vitro* and *in-vivo* models. Consequently, nanoparticles may be supportive in optimized drug delivery to the target cancer area [23,33,34]. The efficiency of copper as antimicrobial and anti-cancer agent has been known for a long time. The bio-potentials of copper nanoparticles are due to their huge aspect ratio compared to the bulk material. These properties allow them to have better retention time and enter into the bacterial cells, as their membranes are in size of nanometer range [35]. Recently, Mali et.al., [28] proposed a green synthesis of C nanoparticles by using *Celastrus paniculatus* leaf extract and evaluated the

antifungal activity against various pathogens. In another report Jahan et.al., [32] studied the antibacterial efficacy of Cu-NPs synthesized by citrus sinensis as bio reductant. A recent report by Noor et. al., [23] claimed the anticancer, antibacterial, antidiabetic properties of fungi mediated by Cu-NPs fabricated by *Aspergilllus niger*. Biresaw et.al., [30] evaluated the anticancer potential of Cu-NPs synthesized by *Prunus nepalensis* leaf extract in breast cancer (MCF-7 cells). The report of Chinnathambi et.al., [34] claimed the chemotherapeutic potential against human endometrial cancer cells and antioxidant properties of green synthesized Cu-NPs by *Allium noeanum* leaves. In another report Jahan et.al., [32] studied the antibacterial efficacy of Cu-NPs synthesized using *Citrus sinensis* as bio reductant.

Borassus flabellifer L. generally identified as palmyra palm, is widely distributed throughout India and tropical Asian countries. Almost all parts of the plant are used in traditional medicine as antidiabetic, antimicrobial, anti-inflammatory, and antioxidant [36,37]. The sap of *B. flabellifer* (pathaneer in Tamil) is widely consumed as a source of palm sugar and its inflorescence produces a sweet sap, which is a popular beverage. The palm sap, syrup, and fruit have shown enormous applications in fermentation. Reshma et al., [38] isolated 2,3,4-trihydroxy-5-methylacetophenone from the palm syrup and claimed that it possessed potent radical scavenging activity. Though there are a handful of reports on green synthesis of copper nanoparticles, to the best of our knowledge there is no report on *Borassus flabellifer* Nectar mediated copper nanostructure. Hence, the present study focuses on green synthesis, characterization and evaluation of biomedical properties of Copper Nanostructure using Palm nectar as bio-reductant as well as bio stabilizing agent.

EXPERIMENTAL SECTION

Materials

All the chemicals viz., Copper sulphate pentahydrate, Sodium potassium tartrate, Sodium hydroxide, etc., were of AnalaR Grade samples obtained from Merck, and used without any further purification. De-ionized water was used for all the experiments.

Collection of Palm Nectar

The fresh palm nectar was collected at Erode, Tamilnadu from palm tree farmers. The calcium enriched palm nectar was centrifuged at 5000 rpm for 5 minutes and subsequently the supernatant was filtered using Whatman No.1 filter paper. The filtrate contains sugars and other phytochemicals were considered as the source of bio-reductant and stabilizing agent.

Synthesis of Palm Nectar mediated Copper Nanostructures

Double distilled water has been used throughout the synthesis. Aqueous solution (0.02 M) of copper sulphate pentahydrate was dissolved in 50 ml distilled water (Fehling A). Subsequently Sodium potassium tartrate and sodium hydroxide were dissolved in 50 ml distilled water (Fehling B). The centrifuged pure palm nectar (25 ml) was taken in a clean beaker containing 75 ml of water. The freshly prepared Fehling's A & B solutions taken in separate burettes were discharged instantaneously drop by drop over a period of 30 minutes to the palm nectar with constant stirring for the germination of copper nanoparticles. Once the contents were dropped into the reaction vessel, an imminent colour change from blue to yellowish green could be observed, which denoted the metal ion reduction, and the entire reaction mixture was continued to be under stirring on the magnetic stirrer for a further 10 minutes - 15 minutes for the completion of the bio-reduction process. The PN-Cu-NS formed were separated out from the solution by centrifugation (6000 rpm, 10 minutes), washed several times with water, methanol, acetone, and vacuum dried, subjected to various physicochemical investigations.

CHARACTERIZATION

Optical properties of the prepared samples were monitored at regular intervals and the absorption maximum was determined by UV-vis spectroscopy, (Agilent technologies Carry 8454, USA) spectrophotometer. Fourier transform infrared (FT-IR) spectrophotometer (Shimadzu - 800 series, Japan) was used for characterizing the prepared samples by KBr method. Powder-X-Ray Diffraction (XRD) patterns were recorded with Philips analytical X-ray diffractometer using Cu Kα radiation (1.54056 A˚). HR-TEM images and SAED patterns for Cu NPs were obtained using a JEOL 2100 LaB6 transmission electron microscope (200 kV). HR-TEM samples were prepared by dropping the colloids onto carbon-coated TEM grids (Carbon Cu grids, Ted Pella, Redding, CA, USA) and allowing the liquid carrier to evaporate in air.

EVALUATION OF ANTIMICROBIAL PROPERTIES

Antibacterial activity (Disc Diffusion Method)

The antimicrobial activity of palm nectar stabilized Copper nanostructures (PN-Cu-NS) was evaluated using disc diffusion method [16]. Accordingly, the bacteria both Gram positive (*Staphylococcus aureus, Bacillus subtilis*) and Gram negative (*Escherichi coli, Pseudomonas aeruginosa*) were inoculated into Muller Hinton broth and incubated at 37°C overnight. Then, 100 µl of primed bacterial suspensions (106 CFU/ml) were cultured on the surface of plates containing Muller Hinton Agar. Then, sterile filter paper disks with diameter of 6 mm were stained with PN-Cu-NS suspension (100 µg/disc) and placed over the surface of the bacterial culture. Ciprofloxacin (10 µg/disc) was used as a standard for comparison. The plates were subsequently incubated at 37°C for 24 hours and finally, the diameter of the growth inhibition zones was measured. Ciprofloxacin antibiotic disc was used as positive control. Minimum inhibitory concentration (MIC) was assessed by dilution in a liquid medium [16]. Accordingly, a dilution series was prepared with 10 ml Nutrient Broth culture medium containing different concentrations of PN-Cu-NS. In the next step, 50 µl of bacterial suspensions (106 CFU/ml) were added to all dilutions. The lowest concentration in which no bacterial growth was observed was determined as the MIC.

Antifungal Activity (Disc Diffusion Method)

The antifungal activity of palm nectar stabilized Copper nanostructure (PN-Cu-NS) was determined against *Candida albicans, Aspergillus niger, Aspergillus fumigates* and *Monococeus purpureces* using disc diffusion method [20]. Prior to the experiment, the filter paper discs were individually saturated with PN-Cu-NS (100 µg/disc) and then aseptically placed on Sabouraud Dextrose Agar medium that had been incubated with the culture. The plates were then incubated at 37°C for 48 hours. Since the incubation time for microbial growth varies between fungi and bacteria. The zone of inhibition was measured (in millimeters) and the means of triplicate samples were recorded.

Evaluation of Antioxidant Activity (DPPH Radical Scavenging Assay)

The antioxidant activity of PN-Cu-NS was evaluated by DPPH free radical scavenging assay. This assay was accomplished according to the method described by Wu et al., [39] Briefly, the PN-Cu-NS was dispersed in methanol at different concentrations (20 µg/ml - 100 µg/ml). About 0.5 ml of dispersed PN-Cu-NS was added to 3 ml of 0.5 mM DPPH in methanol solution and this reaction mixture was incubated for 30 minutes in the dark with consequent shaking in regular interval. The color change of the reaction mixture was observed from purple to yellow indicates that PN-Cu-NS reduced the DPPH by donating a hydrogen atom. The absorbance of the reaction mixture was subsequently measured at 517 nm using a UV-Vis spectrophotometer. The percentage of DPPH inhibition was calculated by using the following formula.

$$\% \text{ of Scavenging} = \frac{\text{OD of Control} - \text{OD of test sample}}{\text{OD of Cotrol}} \times 100 \quad (1)$$

Cytotoxicity Assessment

Cell lines and culture medium

The cell lines were procured from ATCC, stock cells were cultured in DMEM supplemented with 10% inactivated Fetal Bovine Serum (FBS), penicillin (100 IU/ml), streptomycin (100 µg/ml) in a humidified atmosphere of 5% CO_2 at 37°C until confluence. The cells were dissociated with cell dissociating solution (0.2% trypsin, 0.02% EDTA, 0.05% glucose in PBS). The viability of the cells is checked and centrifuged. Further, 50,000 cells/well was seeded in a 96 well plate and incubated for 24 hours at 37°C, 5% CO_2 incubator.

MTT assay

The monolayer cell culture was trypsinized and the cell count was adjusted to 5.0×10^5 cells/ml using respective media containing 10% FBS. To each well of the 96 well micro titer plates, 100 µl of the diluted cell suspension (50,000 cells/well) was added. After 24 hours, when a partial monolayer was formed, the supernatant was flicked off, washed the monolayer once with medium and 100 µl of different test concentrations of test drugs were added on to the partial monolayer in microtiter plates. The plates were then incubated at 37°C for 24 hours in 5% CO_2 atmosphere. After incubation, the supernatant liquids in the wells were discarded and 100 µl of MTT (5 mg/10 ml of MTT in PBS) was added to each well. The plates were incubated for 4 hours at 37°C in 5% CO_2 atmosphere. The supernatant was removed and 100 µl of DMSO was added and the plates were gently shaken to solubilize the formed formazan. The absorbance was measured using a microplate reader at a wavelength of 590 nm. The percentage growth inhibition was calculated using the following formula and concentration of test drug needed to inhibit cell growth by 50 % (IC50) values was generated from the dose-response curves for each cell line [18].

$$\% \text{ Viability} = \frac{\text{OD of Experimental sample}}{\text{OD of Experimental control}} \times 100 \quad (2)$$

RESULTS AND DISCUSSION

UV-Visible Studies

Figure 1 shows the UV-vis absorption spectra of (a) Pure palm nectar, (b) Pure Fehling's solution and (c) PN-Cu-NS. The pure palm nectar shows (Figure 1A) absorption at 280 nm that corresponds to benzoyl systems of phenolic moieties which are related to π-π^* transitions. Therefore, the band observed at UV region corroborates the presence of phenolics in bioresources as reported by literature [5,40,41]. Pure Fehling's solution shows a single broad absorption peak in the region 600 nm - 800 nm (Figure 1B), which is attributed to the d–d transition of Cu^{2+} ions [42]. The formation and stabilization of PN-Cu-NS is confirmed by the surface plasmon resonance absorption spectral peak at 583 nm (Figure 1C) has good agreement with existing literature [14-16]. The formation of Cu-NS might proceed via complex formation of Cu^{2+} -ion with the various reducing sugars and other antioxidant moieties present in PN, followed by intramolecular electron transfer reduction of Cu^{2+} into Cu atom followed by accumulation and stabilization of the Cu-NS [43]. Nanosized Cu particles generally exhibit a surface Plasmon peak at around 556 nm to 600 nm. Some authors claimed the blue shift of the surface plasmon resonance of the metallic nanoparticles with their decreasing size [15]. However, this is not perpetuity the case; some additional effects such as the partial oxidation of colloidal Copper nanoparticles can also be liable for the absorption at shorter wavelengths [14]. Phytoconstituents present in Palm nectar such as Ascorbic acid, a familiar antioxidant with the capability to scavenge free radicals and ROS and it is also a mild reducing agent. As shown in Scheme (Reaction Scheme (1 & 2)), the reactions that lead to the formation of semidehydroascorbate radicals and dehydroascorbic acid are also accompanied by electron-donation processes. Released hydrogen free radicals react with hydroxy free radicals and oxygen that are associated with the oxidation of nanoparticles.

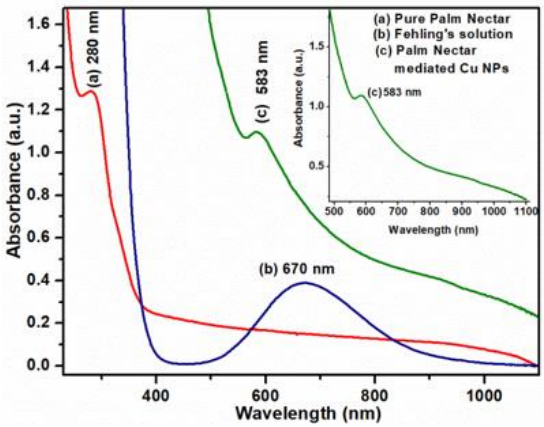

Figure 1: UV-vis. spectra of: **A)** Pure palm nectar; **B)** Pure Fehling's solution; **C)** PN-Cu-NS.

Diffused Reflectance Spectral studies (DRS)

The diffused reflectance spectrum (Figure 2A) depicts that the SPR region at 594 nm with broad shoulder peak around 557 nm is expanded and given in (Figure 2B). Around 10 nm red shift has been found from 583 nm (colloidal state of PN-Cu-NS) to 594 nm (Solid state) is attributed to the oxidation of Cu into its corresponding oxides (Cu_2O and CuO) and core shell formation. The band gap of the PN-Cu-NS is estimated to be 2.17 which clearly depicts the mixed phase of Cu/Cu_2O, also it has good agreement with the existing report [9]. The optical band gap energy of PN-Cu-NS is estimated by Kubelka - Munk function (Equation 3).

$$\boldsymbol{F(R)} = \frac{(1-R^2)}{2R} \qquad (3)$$

The optical band gap energy (E_g) is estimated by plotting $(F(R) \times h\nu)^2$ versus the photon energy ($h\nu$), from the intersection between the linear fit and the photon energy axis [12]. The results revealed that the estimated optical band gap energy is found to be 2.09 eV, for PN-Cu-NS. Since this band gap value is close to that reported for Cu_2O system, we could conclude that the synthesized PN-Cu-NS have considerable amount of Cu_2O as an oxidized product of copper. Moreover, it is also probable that some of Cu_2O can further be oxidized into CuO since the estimated band gap energy is lower than the reported ones. The mixed phases of Cu, Cu_2O and CuO have been further confirmed by XRD analysis and SAED pattern obtained from HR-TEM analysis (Vide-supra).

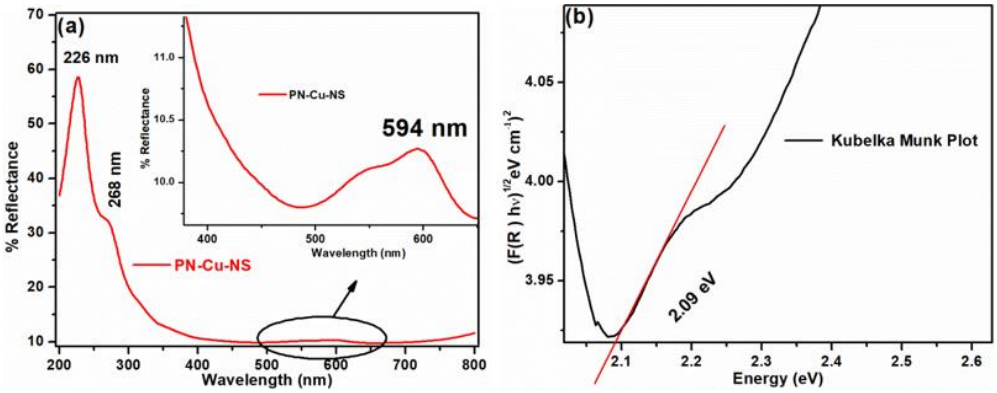

Figure 2: A) DRS spectra (Reflectance) of PN-Cu-NS, **B)** Band gap determination by Kubelka Munk plot.

FT-IR Investigation

Figure 3 depicts the FT-IR spectra of (A) Pure palm nectar and (B) PN-Cu-NS, the various peaks observed in the FT-IR spectra of Copper nanostructure using palm nectar as bio reductants including Vitamin C and other phytochemicals indicates the very strong influence of palm nectar.

It was envisioned that palm nectar plays dual role as reductant followed by capping/protecting agent of virgin Cu nanostructures. The observed peaks at 3375 cm^{-1} and 1651 cm^{-1} mainly attributes to the -OH stretching and bending vibrations. Compared to pure palm nectar the -OH peak shows a shift (3375 cm^{-1} to 3318 cm^{-1}) to lower frequency and a decrease in intensity, which may be due

to the oxygen containing groups such as -OH or -COOH groups associated with the formation of Cu nanostructure [15]. The two bands at 2977 cm^{-1} and 2830 cm^{-1} correspond to -CH2- asymmetric and symmetric stretching frequencies [9]. The peak at 2885 cm^{-1} signifies to -C-H stretching of vitamin C/other phytochemicals. The band at 1419 cm^{-1} might be due to the scissoring, twisting, wagging or deformation modes of -CH2- group. The band in the lower fingerprint region is attributed to the metal / metal oxide nano structures. Though the FT-IR spectra could exhibit a number of prominent and less prominent peaks at various regions impressing the presence of very specific functional groups, there are notable absences of predominant peaks. To cite a few, the absence of any peak between 1900 cm^{-1} - 1600 cm^{-1} indicates that there is carbonyl/C=N/-C=C-/moieties present in the system. This confirms the reduction Cu^{2+} in the Cu nanostructure by vitamin C and other phytochemicals at the expense of rupturing of lactones ring. The absence of prominent peak to be observed around 1720 cm^{-1} - 1730 cm^{-1} might be due to the oxidative cleavage of Vitamin C/Lactonic ring into Gluconic/Glucuronic acid. The IR active mode of Cu_2O bulk system is around 620 cm^{-1}. However, the nanostructure Copper system shows the absorption bands with slight shift to higher wave-number. The new peak appears at 643 cm^{-1} in fingerprint region of PN-Cu-NS may belong to the Cu-O vibration [27,44].

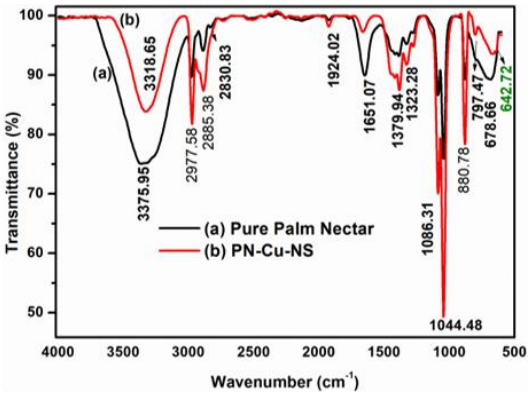

Figure 3: FT-IR spectra of: **A)** Pure palm nectar; **B)** PN-Cu-NS.

Powder X-ray Diffraction Analysis

The crystal nature and phase composition of synthesized copper nanostructure is analyzed by powder XRD technique depicted in Figure 4 and Table 1. The strong and sharp characteristic peaks observed at 2θ = 43.29 (111), 50.40 (200), 74.09 (220) are ascribed to the FCC phase of metallic Copper (marked with clubs' symbol), the obtained result has good agreement with existing literatures (JCPDS: 04-0836) [13, 19]. The reflections in the diffractogram confirmed crystal structure of elemental Cu with lattice constant a = 3.62 A˚ that match well with standard lattice parameter (a = 3.615 A˚) [17,35]. In addition, the peaks observed at 2θ = 29.49 (110), 36.44 (111), 42.32 (200), 61.40 (220), 73.44 (311), 77.37 (222) are corresponding to Cu_2O phase (marked with diamond symbol) (JCPDS: 05-0667) [19]. These peaks ascribed to the formation of BCC crystal structure of Cu_2O with lattice constant a = 4.26 A˚, in concord with the standard data (a = 4.269 A˚). Besides the less intense peaks observed at 32.47 (110), 35.49 (11-1), 38.63 (111), 48.81 (20-2), 53.1 (020), 58.25 (202), 66.36 (31-1), 67.36 (220) are related to CuO phase (marked with spades symbol) (JCPDS: 48-1528). Comparatively the intensity of Cu and Cu_2O phase higher than CuO phase indicating that the PN-Cu-NS is mainly composed of Cu an Cu_2O phases. The XRD diffraction pattern showed the coexistence of three crystalline phases, i.e., metallic Cu, Cu_2O and less amount of CuO. This obviously illustrates that the zero-valent Copper nanoparticles go through decomposition due to limited stability of copper, the derivatives Cu2O and CuO might be formed by oxidation. The size of the Copper nanoparticle is found by using Scherer formula.

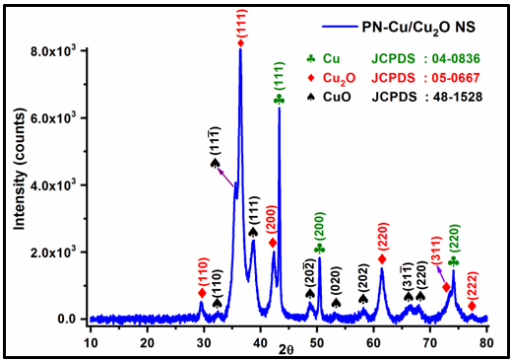

Figure 4: Powder X-ray diffraction pattern of PN-Cu-NS.

S. No.	X-Ray Diffraction Peaks with corresponding d_{hkl} values					
	Cu		Cu_2O		CuO	
	2θ (°)	d_{hkl}	2θ (°)	d_{hkl}	2θ (°)	d_{hkl}
1.	43.29	(111)	29.49	(110)	32.47	(110)
2.	50.40	(200)	36.44	(111)	35.49	(11-1)
3.	74.09	(220)	42.32	(200)	38.63	(111)
4.			61.40	(220)	48.81	(20-2)
5.			73.44	(311)	53.1	(020)
6.			77.37	(222)	58.25	(202)
7.					66.36	(31-1)
8.					67.36	(220)

Table 1: Powder X-Ray Diffraction peaks with $d_{(hkl)}$ values.

Morphological Characterization

FE-SEM analysis

Figure 5A and figure 5B shows the FE-SEM micrographs of PN-Cu-NS and revealing a lot of stacked hallow like spheres and deformed spherical clusters with almost uniform diameters. Phytoconstituents present in Palm nectar ensure the regular and uniform size distribution of nanoparticles by preventing further agglomeration. Higher magnification of FE-SEM image (Figure 5B) shows the well-defined surface modification and coating of biomolecules, which stabilize the fine surface of copper nanostructure. These hollow structures are composed of small nanoparticles, making holes on the surface. EDAX analysis (Figure 5C) shows that the PN-Cu-NS contains Cu and O elements, total weight percent of copper and oxygen atoms are found to be 78.19%, 21.81% respectively.

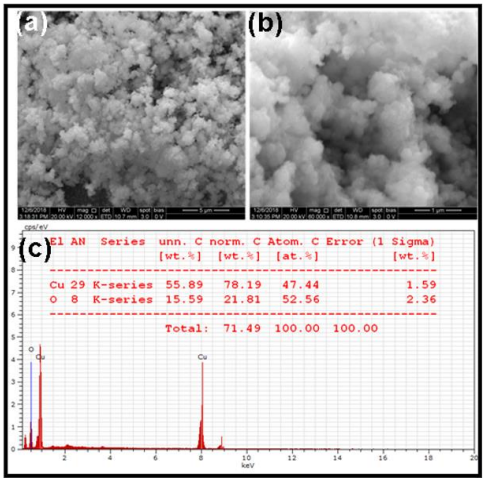

Figure 5: A & B) FE-SEM images of PN-Cu-NS; **C)** EDX spectrum.

HR-TEM analysis

The structure and particle size of PN-Cu-NS was analyzed using HR-TEM (Figure 6). The obtained micrographs expose well dispersed spherical Copper nanostructure with average diameter of 50 nm - 200 nm. The selected area diffraction pattern of CuNPs shown in Figure 6D, revealing that the face centered poly crystalline structure of copper nanoparticles. The d spacing of inner lattice fringes (Figure 6C) CuNPs is estimated as 0.2602 nm, which is in good agreement with the value of (111) plane of FCC Cu as derived from XRD data (vide supra).

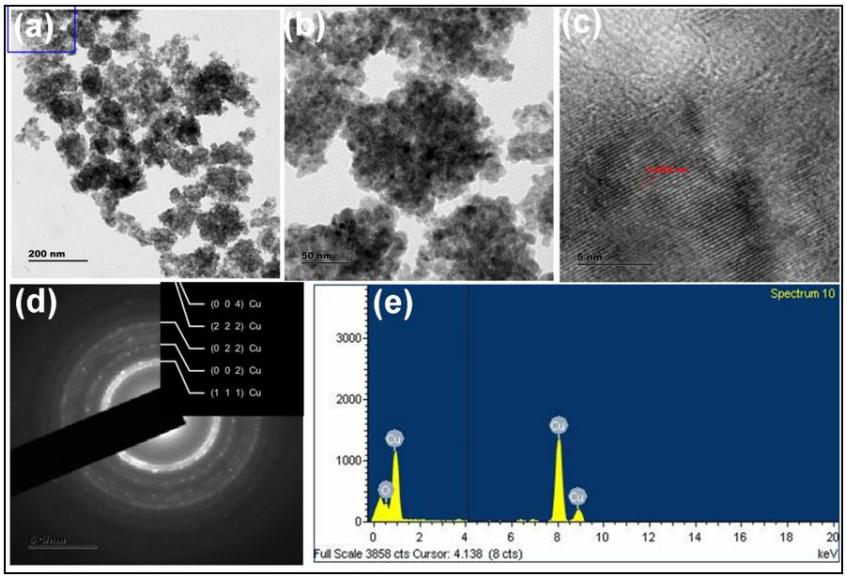

Figure 6: A & B) HR-TEM image with different magnifications; **C)** Lattice fringes; **D)** SAED pattern; **E)** EDX spectra of PN-Cu-NS.

BIOLOGICAL APPLICATIONS

Anti-Bacterial Activity

The disk diffusion method was employed to investigate the antibacterial potential of the PN-Cu-NS against *Staphylococcus aureus, Bascillus subtilis, Escherichia coli* and *Pseudomonas aeruginosa*. PN-Cu-NS showed zone of inhibition as indicated in Figure 7 and Table 2. Maximum zone of inhibition obtained in Gram positive bacterial strain (*Staphylococcus aureus*) with a zone diameter of 32 mm at a concentration of 100 µg/ml and lowest zone of inhibition was observed in Gram negative bacteria (*Pseudomonas aeruginosa*) with a zone diameter of 13 mm at same concentration. The minimum inhibitory concentration (MIC) of PN-Cu-NS of bacteria *Staphylococcus aureus* 250 µg/ml and *Escherichia coli* 125 µg/ml. the occurrence of an inhibition zone clearly indicates the antimicrobial potential of PN-Cu-NS.

Although the PN-Cu-NS demonstrated its antibacterial potential against both Gram-positive and Gram-negative bacteria, it was found that the antibacterial effects of PN-Cu-NS were elevated in case of Gram-positive (*S. aureus* and *B. subtilis*) bacteria than the Gram-negative (*E. coli.* and *P. aeruginosa*) bacterial strains, with the inhibition zones of 32 mm, 15 mm 16 mm and 13 mm, respectively (Table 2). From the preceding reports it was observed that Copper nanoparticles tending the depolarization of the bacterial cell membrane which engendered the cell filamentation. Besides, Cu nanoparticles also spectacularly amplified the cellular ROS level which affected protein oxidation, lipid peroxidation, and produce DNA degradation; and lastly, killed the bacterial cells [32]. The anti-bacterial activity of PN-Cu-NS is the size of nanoparticles that plays a vital role in inhibition of bacterial growth; especially the high aspect ratio improves the interaction with the bacteria and increases the antibacterial efficacy. Correspondingly, tiny particle size increases the release of metal ions from the surface of the nanoparticles and gives mount to added antibacterial properties. Hence, the antibacterial properties of PN-Cu-NS may be attributed to their relatively small size. Even though the antimicrobial mechanisms of metallic nanoparticles are not completely understood, three mechanisms have been reported in various sources: (1) The accumulation and dissolution of metal nanoparticles in the bacterial membrane changes permeability and consequently releases lipopolysaccharides, membrane proteins and intracellular biomolecules, and vanish proton drive force in the plasma membrane. (2) The creation of reactive oxygen species that results in oxidative damage to the cell structure. (3) Absorption of metallic ions derived from nanoparticles, which leads to reduced intracellular ATP levels and impaired DNA replication [16].

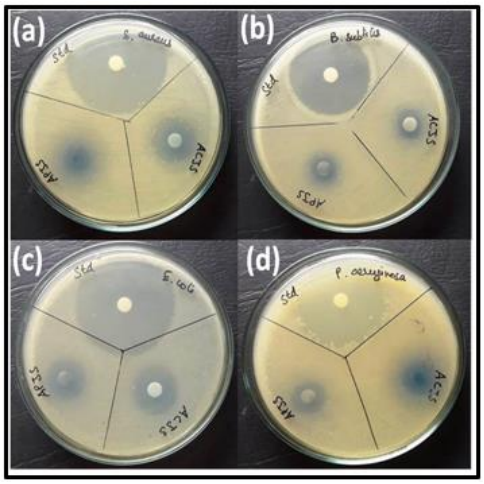

Figure 7: Antibacterial activities of PN-Cu-NS against (A) *S. aureus*; (B) *B. subtilis*; (C) *E. coli*; and (D) *P. aeruginosa*.

S. No.	Bacterial Pathogens	Zone of Inhibition (mm) Mean		MIC (µg/ml)
		Standard (Ciprofloxacin) (10 µg/disc)	PN-Cu-NS (100 µg/disc)	
1.	*Staphylococcus aureus*	45	32	250
2.	*Bacillus subtilis*	38	15	
3.	*Escherichia coli*	43	16	125
4.	*Pseudomonas aeruginosa*	42	13	

Table 2: Antibacterial activity of palm nectar mediated copper nanostructure (PN-Cu-NS).

Anti-Fungal Activity

The anti-fungal activity of PN-Cu-NS against *Candida albicans*, *Aspergillus niger*, *Aspergillus fumigates* and *Monococeus purpureces* was executed using the protocol from CLSI and the observed results displayed good antifungal activity on all the strains, which matched with standard Ciprofloxacin (Figure 8 and Table 3). The maximum zone of inhibition was observed in Candida albicans with zone diameter 13 mm at the concentration of 100µg/ml and the zone diameter 9 mm in *Aspergillus niger*, *Aspergillus fumigates* and *Monococeus purpureces*. The MIC value was found to be 250 µg/ml against *Candida albicans*, these Cu NPs play a major role in cytoplasmic damage in fungi which resulting in apoptosis of fungal strains. The results undoubtedly depict that the PN-Cu-NS can act as better fungicidal agent compared to commercially available standard.

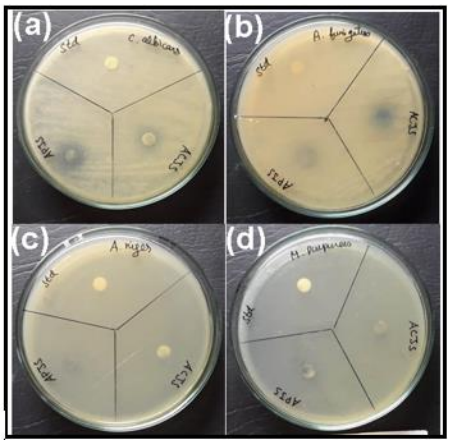

Figure 8: Antifungal activities of PN-Cu-NS against A) *C. albicans*; B) *A. fumigates*; C) *A. niger* and D) *M. purpureces*.

S. No.	Name of the Fungi	Zone of Inhibition (mm) Mean	
		Standard (Ciprofloxacin) (10 µg/disc)	PN-Cu-NS (100 µg/disc)
1.	*Candida albicans*	9	13
2.	*Aspergillus Niger*	10	9
3.	*Aspergillus fumigates*	9	9
4.	*Monococeus purpureces*	9	9

Table 3: Antifungal activity of the PN-Cu-NS.

Assessment of Antioxidant Activity of PN-Cu-NS through DPPH Radical Scavenging Assay

Antioxidant activity is one of the most important applications of nanomaterials. In biological systems, free radicals are generated as a result of the interaction of biomolecules with molecular oxygen. Moreover, antioxidants have been known as therapeutic agents with antitumor, anti-inflammatory, anti-mutagenic, anti-cancer, antimicrobial and anti-atherosclerotic properties [22]. The antioxidant activity of PN-Cu-NS was investigated by UV-vis. absorbance spectroscopy using DPPH as a stable free radical (Figure 9). The half inhibitory concentration (IC_{50}) value for the PN-Cu-NS is found to be 46.9 µg/ml (Figure 9). Dashtizadeh et al., [45] studied the antioxidant activity of *Prunus mahaleb L* mediated Copper nanoparticles and they found very low antioxidant activity around 15.90% even at higher concentration (2 mg/ml). Many studies reported that biosynthesized copper nanoparticles have strong antioxidant activity at low concentration [1,39,46].

The obtained results corroborated that the PN-Cu-NS have very high antioxidant activity and it is strongly recommended this application of natural antioxidant for health protection beside different oxidative stress related to degenerative diseases. The possible mechanism behind the radical scavenging of DPPH· by PN-Cu-NS is due to the odd electron, DPPH shows a strong absorption band at 517 nm in the visible spectrum. The absorption decreases as the odd electron becomes paired off in the presence of a free radical scavenger (bio-molecules tethered on PN-Cu-NS) [47]. By accepting one electron from the PN-Cu-NS, the DPPH· becomes DPPH- anion and it further converted as DPPH-H by accepting one proton from PN-Cu-NS. This suggested two step mechanisms for the scavenging reaction of DPPH, electron accepting in the first step followed by proton capture in the second step [48].

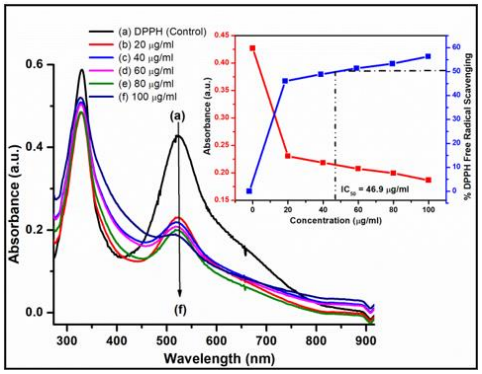

Figure 9: DPPH radical scavenging activity of PN-Cu-NS (percentage of inhibition).

Cytotoxicity of PN-Cu-NS in A549 Cells and HeLa Cells

The *in-vitro* anticancer activity of the green synthesized PN-Cu-NS was evaluated against human cancer cell lines such as lung cancer cells (A549) and cervical cancer cells (HeLa) by MTT assay using doxorubicin as standard anti-cancer drug. The MTT assay has been extensively employed to evaluate the cell proliferation rate based on the mitochondrial diminution of the tetrazolium salt by actively growing cells to produce blue water insoluble formazan crystals. In the present cytotoxicity analysis, various concentrations (5 µg/ml to 50 µg/ml against A549 cells and 10 µg/ml to 320 µg/ml against HeLa cells) of PN-Cu-NS were tested for 48 hours in triplicates and the results are expressed as an average standard ± deviation and a blank sample was taken as a control to identify the activity of the solvent. The cell viability was concentration dependent, which decreased with increase in concentration of the samples (Figure 10 and Figure 11). The concentration dependent curves of the PN-Cu-NS showed prominent cytotoxicity on both cancer cell lines. The cytotoxicity of the synthesized nanoparticles was relatively low when compared to doxorubicin. A recent report by Rehana et. al., [18] explored the anticancer potential of CuO nanoparticles against a panel of human cancer cell lines as well as normal cell lines. They found that green synthesized CuO NPs show high cytotoxicity in cancerous cell lines especially in A549 cells (IC50 = 20.15 µg/ml ± 1.22 µg/ml) whereas less cytotoxicity in normal cell line. In the present study, the IC50 value of PN-Cu-NS was found to be 12 µg/ml ± 1.2 µg/ml which supports that the anticancer potential of PN-Cu-NS against A549 cells.

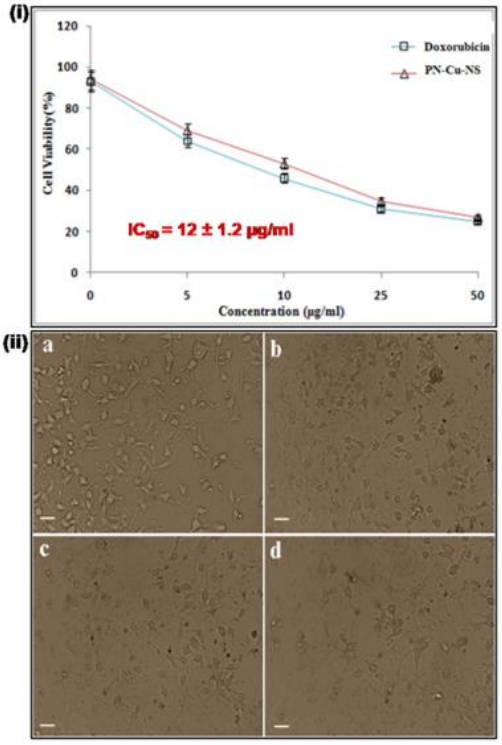

Figure 10: (I) Cytotoxicity of PN-Cu-NS; **(II)** Phase contrast images of: **A)** Control; **B)** 5 µg/ml; **C)** 10 µg/ml; **D)** 25 µg/ml of PN-Cu-NS treated A549 cells.

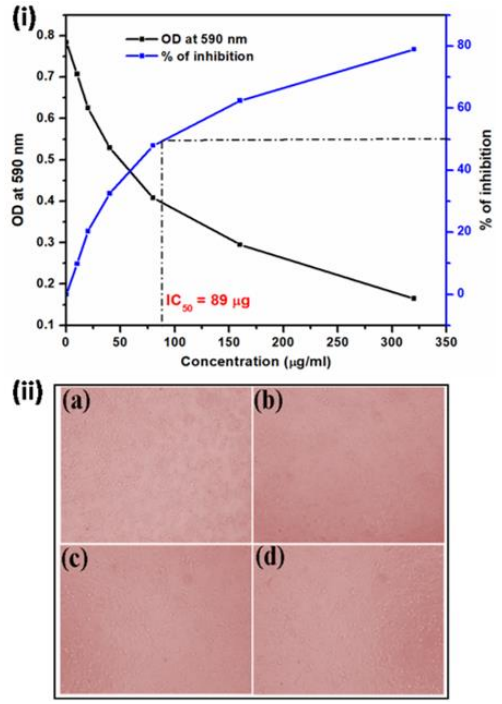

Figure 11: (I) Cytotoxicity profile of PN-Cu-NS; **(II)** Phase contrast images of: **A)** Control; **B)** 25 µg/ml; **C)** 50 µg/ml; **D)** 100 µg/ml of PN-Cu-NS treated HeLa cells.

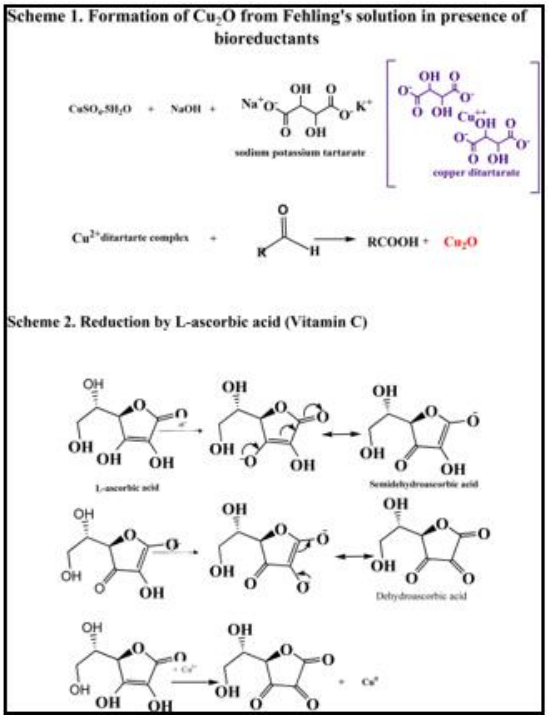

Reaction Scheme: Palm nectar mediated synthesis of Cu/Cu_2O Nanostructures.

CONCULUSION

Palm nectar mediated Copper nanostructure was successfully synthesized by a green method. The green synthesized PN-Cu-NS was characterized by various physiochemical techniques. The FT-IR spectra showed the interaction of phytoconstituents with copper nanostructure. While the powder XRD, FE-SEM, HR-TEM and SAED patterns confirm the Copper nanostructure with its derivatives such as Cu_2O and CuO mixed phase. The biological potential of PN-Cu-NS was evaluated by anti-bacterial activity, anti-fungal activity, antioxidant activity and anticancer activity. The PN-Cu-NS exhibited high antibacterial activity against Gram positive bacterial strains compared to Gram negative bacterial strains. The antifungal activity was evaluated against four different pathogens, where *Candida albicans* showed appreciable zone of inhibition. Moreover, the PN-Cu-NS exhibited extraordinary antioxidant activity (46.9 µg/ml). Furthermore, the PN-Cu-NS explored a promising anticancer activity against A549 cells (12 µg/ml ± 1.2 µg/ml) and HeLa cells (89 µg/ml). The present study clearly shows that palm nectar mediated Copper nanostructure as potential agent for biomedical applications.

ACKNOWLEDGMENT

One of the Authors (Dr. A.R.) thankfully acknowledges the University Grants Commission (UGC), New Delhi and TANSCHE, Chennai for financial assistants in the form of UGC Major Research Project (File No: 39-723/2010 (SR); Dated 11-01-2011) and TANSCHE Minor Research Project Scheme (RC. No. 2026/2020A, Dt. 01.02.2021). I do extend my thanks to Dr. V. Kalaiselvi (PRINCIPAL), Dr. K. Chitra, (our previous Principal; presently Principal, Arignar Anna Government Arts College, Attur - 636121, Tamil Nadu, INDIA), Prof. Joseph Clement, (Former Professor & Head, P.G., & Res. Dept. Botany), and Dr. M. Muthukumar (P.G., & Res. Dept. English), Government Arts College (Autonomous), Coimbatore - 18, for their constant encouragements and valuable discussions. We do extend our warm gratitude to Dr. M. Paulpandi, Department of Proteomics, Bharathiar University, Coimbatore - 46 for his help in carrying out certain biological studies. The Authors are very much grateful to Prof. M. Klinger, Institute of Physics, Prague, Na Slovance, Czech Republic for sharing the CrysTBox Software for interpreting the HR-TEM SAED pattern.

CONFLICT OF INTEREST

The authors claim no conflicts of interest.

REFERENCES

1. Velidandi A, Pabbathi NPP, Dahariya S, et al. (2020) Catalytic and eco-toxicity investigations of bio-fabricated monometallic nanoparticles along with their anti-bacterial, anti-inflammatory, anti-diabetic, anti-oxidative and anti-cancer potentials. Colloid and Interface Science Communications 38: 100302.

2. Makvandi P, Wang CY, Zare EN, et al. (2020) Metal-based nanomaterials in biomedical applications: Antimicrobial activity and cytotoxicity aspects. Advanced Functional Materials 30(22): 1910021.
3. Azharuddin M, Zhu GH, Das D, et al. (2019) A repertoire of biomedical applications of noble metal nanoparticles. Chemical Communications 55(49): 6964-6996.
4. Murthy S, Effiong P, Fei CC (2020) Metal oxide nanoparticles in biomedical applications. In Metal Oxide Powder Technologies: 233-251.
5. Nasrollahzadeh M, Issaabadi Z, Sajadi SM (2018) Green synthesis of a Cu/MgO nanocomposite by Cassytha filiformis L. extract and investigation of its catalytic activity in the reduction of methylene blue, congo red and nitro compounds in aqueous media. RSC Advances 8(7): 3723-3735.
6. Gong S, Wu X, Zhang J, et al. (2018) Facile solution synthesis of Cu 2 O–CuO–Cu (OH) 2 hierarchical nanostructures for effective catalytic ozone decomposition. CrystEngComm 20(22): 3096-3104.
7. Zhuang X, Han C, Zhang J, et al. (2021) Cu/Cu2O heterojunctions in carbon framework for highly sensitive detection of glucose. Journal of Electroanalytical Chemistry 882: 115040.
8. Li Z, Xie G, Wang C, et al. (2021) Binder free Cu2O/CuO/Cu/Carbon-polymer composite fibers derived from metal/organic hybrid materials through electrodeposition method as high performance anode materials for lithium-ion batteries. Journal of Alloys and Compounds 864: 158585.
9. Mousavi-Kamazani M, Zarghami Z, Rahmatolahzadeh R, et al. (2017) Solvent-free synthesis of Cu-Cu2O nanocomposites via green thermal decomposition route using novel precursor and investigation of its photocatalytic activity. Advanced Powder Technology 28(9): 2078-2086.
10. Asthana S, Samanta C, Voolapalli RK, et al. (2017) Direct conversion of syngas to DME: Synthesis of new Cu-based hybrid catalysts using Fehling's solution, elimination of the calcination step. Journal of Materials Chemistry A 5(6): 2649-2663.
11. Yan J, Wang H, Jin B, et al. (2021) Cu-MOF derived Cu/Cu2O/C nanocomposites for the efficient thermal decomposition of ammonium perchlorate. Journal of Solid State Chemistry 297: 122060.
12. El-Berry MF, Sadeek SA, Abdalla AM, et al. (2021) Microwave-assisted fabrication of copper nanoparticles utilizing different counter ions: An efficient photocatalyst for photocatalytic degradation of safranin dye from aqueous media. Materials Research Bulletin 133: 111048.
13. Chen W, Fan Z, Lai Z (2013) Synthesis of core–shell heterostructured Cu/Cu 2 O nanowires monitored by in situ XRD as efficient visible-light photocatalysts. Journal of Materials Chemistry A 1(44): 13862-13868.
14. Tokarek K, Hueso JL, Kuśtrowski P, et al. (2013) Green synthesis of chitosan-stabilized copper nanoparticles. European Journal of Inorganic Chemistry 2013(28): 4940-4947.
15. Al-Enizi AM, Ahamad T, Al-Hajji AB, et al. (2018) Cellulose gum and copper nanoparticles based hydrogel as antimicrobial agents against urinary tract infection (UTI) pathogens. International journal of biological macromolecules 109: 803-809.
16. Hasheminya SM, Dehghannya J (2020) Green synthesis and characterization of copper nanoparticles using Eryngium caucasicum Trautv aqueous extracts and its antioxidant and antimicrobial properties. Particulate Science and Technology 38(8): 1019-1026.
17. Ismail MIM (2020) Green synthesis and characterizations of copper nanoparticles. Materials Chemistry and Physics 240: 122283.

18. Rehana D, Mahendiran D, Kumar RS, et al. (2017) Evaluation of antioxidant and anticancer activity of copper oxide nanoparticles synthesized using medicinally important plant extracts. Biomedicine & Pharmacotherapy 89: 1067-1077.
19. Serra A, Gómez E, Michler J, et al. (2021) Facile cost-effective fabrication of Cu@ Cu2O@ CuO–microalgae photocatalyst with enhanced visible light degradation of tetracycline. Chemical Engineering Journal 413: 127477.
20. Chawla P, Kumar N, Bains A, et al. (2020) Gum arabic capped copper nanoparticles: Synthesis, characterization, and applications. International Journal of Biological Macromolecules 146: 232-242.
21. Sriramulu M, Shanmugam S, Ponnusamy VK (2020) Agaricus bisporus mediated biosynthesis of copper nanoparticles and its biological effects: An in-vitro study. Colloid and Interface Science Communications 35: 100254.
22. Hasanin M, Al Abboud MA, Alawlaqi MM, et al. (2022) Ecofriendly synthesis of biosynthesized copper nanoparticles with starch-based nanocomposite: Antimicrobial, antioxidant, and anticancer activities. Biological Trace Element Research 200(5): 2099-2112.
23. Noor S, Shah Z, Javed A, et al. (2020) A fungal based synthesis method for copper nanoparticles with the determination of anticancer, antidiabetic and antibacterial activities. Journal of Microbiological Methods 174: 105966.
24. Hassan SED, Salem SS, Fouda A, et al. (2018) New approach for antimicrobial activity and bio-control of various pathogens by biosynthesized copper nanoparticles using endophytic actinomycetes. Journal of Radiation Research and Applied Sciences 11(3): 262-270.
25. Yuan M, Guo X, Pang H (2021) Derivatives (Cu/CuO, Cu/Cu2O, and CuS) of Cu superstructures reduced by biomass reductants. Materials Today Chemistry 21: 100519.
26. Chowdhury R, Khan A, Rashid MH (2020) Green synthesis of CuO nanoparticles using Lantana camara flower extract and their potential catalytic activity towards the aza-Michael reaction. RSC Advances 10(24): 14374-14385.
27. Ashraf H, Anjum T, Riaz S, et al. (2021) Inhibition mechanism of green-synthesized copper oxide nanoparticles from Cassia fistula towards Fusarium oxysporum by boosting growth and defense response in tomatoes. Environmental Science: Nano 8(6): 1729-1748.
28. Mali SC, Dhaka A, Githala CK, et al. (2020) Green synthesis of copper nanoparticles using Celastrus paniculatus Willd. leaf extract and their photocatalytic and antifungal properties. Biotechnology Reports 27: e00518.
29. Ghosh MK, Sahu S, Gupta I, et al. (2020) Green synthesis of copper nanoparticles from an extract of Jatropha curcas leaves: Characterization, optical properties, CT-DNA binding and photocatalytic activity. RSC Advances 10(37): 22027-22035.
30. Biresaw SS, Taneja P (2022) Copper nanoparticles green synthesis and characterization as anticancer potential in breast cancer cells (MCF7) derived from Prunus nepalensis phytochemicals. Materials Today: Proceedings 49: 3501-3509.
31. Chen J, Mao S, Xu Z, et al. (2019) Various antibacterial mechanisms of biosynthesized copper oxide nanoparticles against soilborne Ralstonia solanacearum. RSC Advances 9(7): 3788-3799.
32. Jahan I, Erci F, Isildak I (2021) Facile microwave-mediated green synthesis of non-toxic copper nanoparticles using Citrus sinensis aqueous fruit extract and their antibacterial potentials. Journal of Drug Delivery Science and Technology 61: 102172.
33. Yaqub A, Malkani N, Shabbir A, et al. (2020) Novel biosynthesis of copper nanoparticles using Zingiber and Allium sp. with synergic effect of doxycycline for anticancer and bactericidal activity. Current Microbiology 77(9): 2287-2299.

34. Chinnathambi A, Awad Alahmadi T, Ali Alharbi S (2021) Biogenesis of copper nanoparticles (Cu-NPs) using leaf extract of Allium noeanum, antioxidant and in-vitro cytotoxicity. Artificial Cells, Nanomedicine, and Biotechnology 49(1): 500-510.
35. Pariona N, Mtz-Enriquez AI, Sánchez-Rangel D, et al. (2019) Green-synthesized copper nanoparticles as a potential antifungal against plant pathogens. RSC Advances 9(33): 18835-18843.
36. Pammi N, Bhukya KK, Lunavath RK, et al. (2021) Bioprospecting of palmyra palm (Borassus Flabellifer) nectar: Unveiling the probiotic and therapeutic potential of the traditional rural drink. Frontiers in Microbiology: 1737.
37. Tusskorn O, Pansuksan K, Machana K (2021) Borassus flabellifer L. crude male flower extracts alleviate cisplatin-induced oxidative stress in rat kidney cells. Asian Pacific Journal of Tropical Biomedicine 11(2): 81-88.
38. Reshma MV, Jacob J, Syamnath VL, et al. (2017) First report on isolation of 2, 3, 4-trihydroxy-5-methylacetophenone from palmyra palm (Borassus flabellifer Linn.) syrup, its antioxidant and antimicrobial properties. Food Chemistry 228: 491-496.
39. Wu S, Rajeshkumar S, Madasamy M, et al. (2020) Green synthesis of copper nanoparticles using Cissus vitiginea and its antioxidant and antibacterial activity against urinary tract infection pathogens. Artificial Cells, Nanomedicine, and Biotechnology 48(1): 1153-1158.
40. Boulet JC, Ducasse MA, Cheynier V (2017) Ultraviolet spectroscopy study of phenolic substances and other major compounds in red wines: Relationship between astringency and the concentration of phenolic substances. Australian Journal of Grape and Wine Research 23(2): 193-199.
41. Nasrollahzadeh M, Maham M, Rostami-Vartooni A, et al. (2015) Barberry fruit extract assisted in situ green synthesis of Cu nanoparticles supported on a reduced graphene oxide-Fe_3O_4 nanocomposite as a magnetically separable and reusable catalyst for the O-arylation of phenols with aryl halides under ligand-free conditions. RSC Advances 5(79): 64769-64780.
42. Hörner TG, Klüfers P (2016) The species of Fehling's solution. European Journal of Inorganic Chemistry 2016(12): 1798-1807.
43. Cheirmadurai K, Biswas S, Murali R, et al. (2014) Green synthesis of copper nanoparticles and conducting nanobiocomposites using plant and animal sources. RSC Advances 4(37): 19507-19511.
44. Guo D, Wang L, Du Y, et al. (2015) Preparation of octahedral Cu_2O nanoparticles by a green route. Materials Letters 160: 541-543.
45. Dashtizadeh Z, Kashi FJ, Ashrafi M (2021) Phytosynthesis of copper nanoparticles using Prunus mahaleb L. and its biological activity. Materials Today Communications 27: 102456.
46. Muthuvel A, Jothibas M, Manoharan C (2020) Synthesis of copper oxide nanoparticles by chemical and biogenic methods: Photocatalytic degradation and in vitro antioxidant activity. Nanotechnology for Environmental Engineering 5(2): 1-19.
47. Paul SS, Selim M, Saha A, et al. (2014) Synthesis and structural characterization of dioxomolybdenum and dioxotungsten hydroxamato complexes and their function in the protection of radiation induced DNA damage. Dalton Transactions 43(7): 2835-2848.
48. Tabrizi L, Dao DQ, Vu TA (2019) Experimental and theoretical evaluation on the antioxidant activity of a copper (ii) complex based on lidocaine and ibuprofen amide-phenanthroline agents. RSC Advances 9(6): 3320-3335.